



LAWRENCE  
LIVERMORE  
NATIONAL  
LABORATORY

# High Speed Measurements using Fiber-optic Bragg Grating Sensors

J. J. Benterou, C. A. May, E. Udd, S. J. Mihailov,  
P. Lu

March 30, 2011

2011 SPIE Defense, Security, & Sensing Conference  
Orlando, FL, United States  
April 25, 2011 through April 29, 2011

## **Disclaimer**

---

This document was prepared as an account of work sponsored by an agency of the United States government. Neither the United States government nor Lawrence Livermore National Security, LLC, nor any of their employees makes any warranty, expressed or implied, or assumes any legal liability or responsibility for the accuracy, completeness, or usefulness of any information, apparatus, product, or process disclosed, or represents that its use would not infringe privately owned rights. Reference herein to any specific commercial product, process, or service by trade name, trademark, manufacturer, or otherwise does not necessarily constitute or imply its endorsement, recommendation, or favoring by the United States government or Lawrence Livermore National Security, LLC. The views and opinions of authors expressed herein do not necessarily state or reflect those of the United States government or Lawrence Livermore National Security, LLC, and shall not be used for advertising or product endorsement purposes.

# High speed measurements using fiber-optic Bragg gratings

Jerry Benterou and Chadd May

Lawrence Livermore National Laboratory, 7000 East Avenue, Livermore, California 94550

Eric Udd

Columbia Gorge Research, LLC, 2555 NE 205<sup>th</sup> Avenue, Fairview, Oregon 97024

Stephen J. Mihailov and Ping Lu

Communication Research Centre-Canada, 3701 Carling Avenue, Ottawa K2H8S2

## ABSTRACT

Fiber grating sensors may be used to monitor high-speed events that include catastrophic failure of structures, ultrasonic testing and detonations. This paper provides insights into the utility of fiber grating sensors to measure structural changes under extreme conditions. An emphasis is placed on situations where there is a structural discontinuity. Embedded chirped fiber Bragg grating (CFBG) sensors can track the very high-speed progress of detonation waves (6-9 km/sec) inside energetic materials. This paper discusses diagnostic instrumentation and analysis techniques used to measure these high-speed events.

Keywords: Fiber gratings, structures, failure, high-speed, detonation velocity, Bragg effect, CFBG

## 1. Introduction

Fiber grating sensors have been used to support measurements on bridges and highways to determine such parameters as vehicle weight, type and speed [1-12]. In this first case, bandwidths that are on the order of 3 to 5 kHz are sufficient to obtain good data. There are cases however where structures fail catastrophically and higher speed systems are required. In this second case, ultrasonic detection in metals and composites require frequencies in the 300 kHz to 5 MHz regime. The considerations associated with these higher speeds involve the length and orientation of the fiber gratings in the structure. The third case involves very high speeds associated with the detonation of energetic materials. In this case, the operational speed of the system ranges from 100 MHz to over 1 GHz. This paper is intended to complement and extend an earlier invited paper on using fiber gratings to support high-speed measurements [20].

## 2. Structural monitoring up to 40 MHz

One of the earliest demonstrations of monitoring structural failure involved the usage of fiber gratings to monitor fiberglass utility poles [13-15]. This was done using a series of high-speed read out systems. The first used an overcoupled coupler technique shown in Figure 1. Here a broadband light source that might be a light emitting diode is used to illuminate a fiber grating that is embedded in a critical area of the utility pole such as the joint area where overloading could result in failure. The light from the fiber grating is directed back to the central beamsplitter and a portion of this light beam is directed toward an overcoupled coupler that has strong wavelength dependence. The first overcoupled couplers had a coupling region of about 10 cm in length and completely transitioned between transmitting and cross coupling light at 1300 nm over a period of about 10 nm. The spectral output of one of the output legs of one of the first overcoupled couplers used is shown in Figure 2. By centering the fiber grating

spectrum between to peak and minimum transmission the ratio of the output detectors could be used to determine the strain on the pole as illustrated by Figure 3.

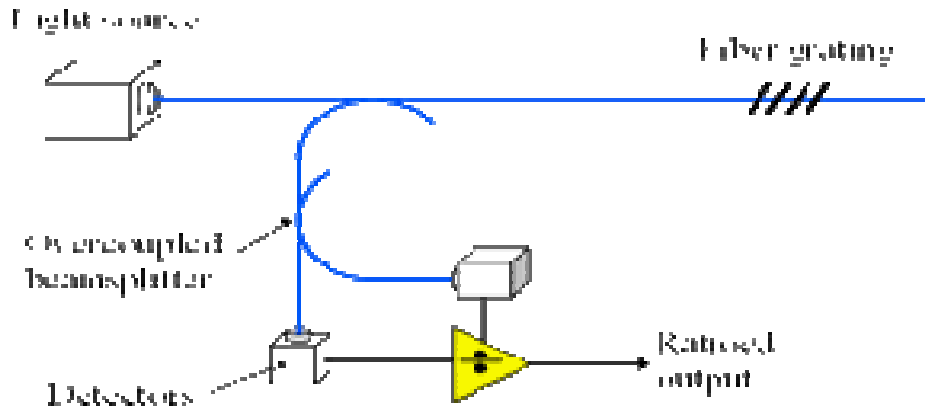


Figure 1 Block diagram of a high speed fiber grating read out system to measure catastrophic failure in a composite utility pole

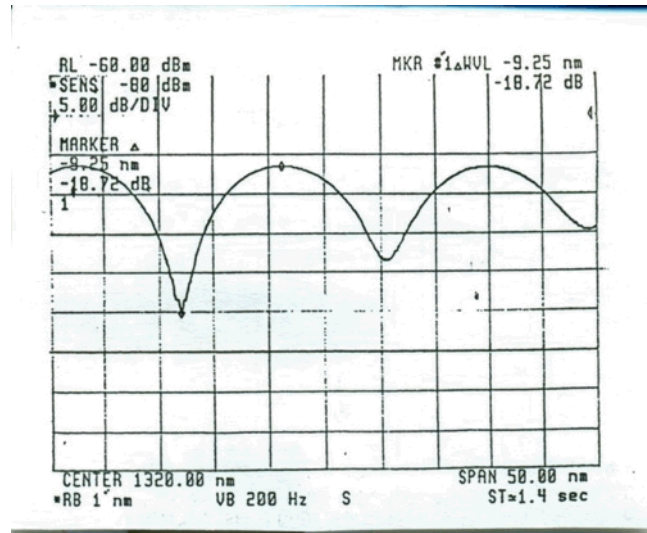


Figure 2 Spectral output of an overcoupled coupler approximately 10 cm in length in the 1300 nm band

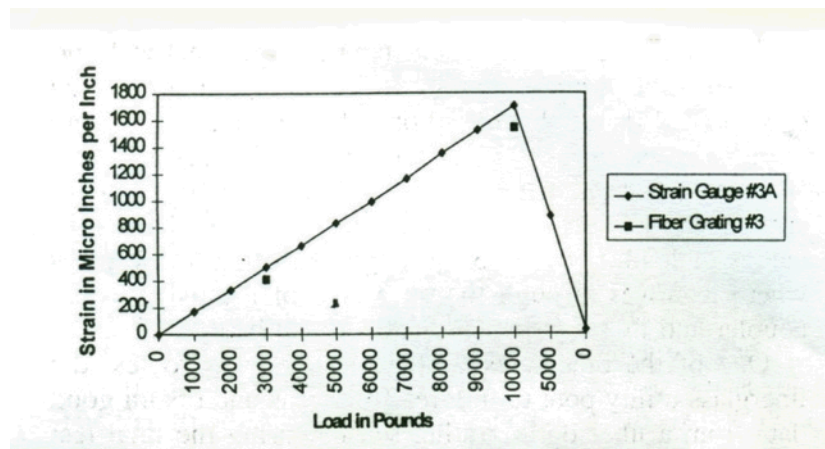


Figure 3 Response of a fiber grating strain sensor through failure of a composite utility pole

The first major tests were performed using a fiberglass utility pole in two sections that was approximately 8 m in length and 30 cm in diameter. Larger utility poles were later manufactured and tested that were a little less than 20 m in length (see Figure 4). The poles were loaded to failure with several fiber grating sensors in place to monitor the composite near the bonded junctions. The recording electronics used had a bandwidth of 10 kHz. The overcoupled coupler was replaced in later systems by the miniature Mach-Zehnder interferometer because it had better temperature stability and less polarization dependence. Chirped gratings mounted on thermally stabilized substructures replaced this later. This approach had better thermal stability than the miniature Mach-Zehnder and was lower cost. The miniature Mach-Zehnder did have the advantage of a very smooth transfer function. This high-speed system was used later to monitor acoustic signals in composite pressure vessels and during ultrasonic tests at speeds up to 1 MHz. It was also used to monitor strain fields induced by high-speed impacts on thick composites up to 30 MHz.



**Figure 4** High speed fiber grating system based on overcoupled coupler and testing of 20 m fiber glass utility pole through failure

At low speeds associated with most civil structures the length of the fiber grating is quite small compared to the acoustic waves generated by structural failure. However at higher speeds associated with ultrasonic detection and high-speed impacts operating frequencies may range from a few hundred kHz up to 10s of MHz [16]. At these frequencies acoustic waves start to have lengths that are comparable to the fiber grating and the orientation of the fiber grating relative to the acoustic wave propagation direction becomes important.

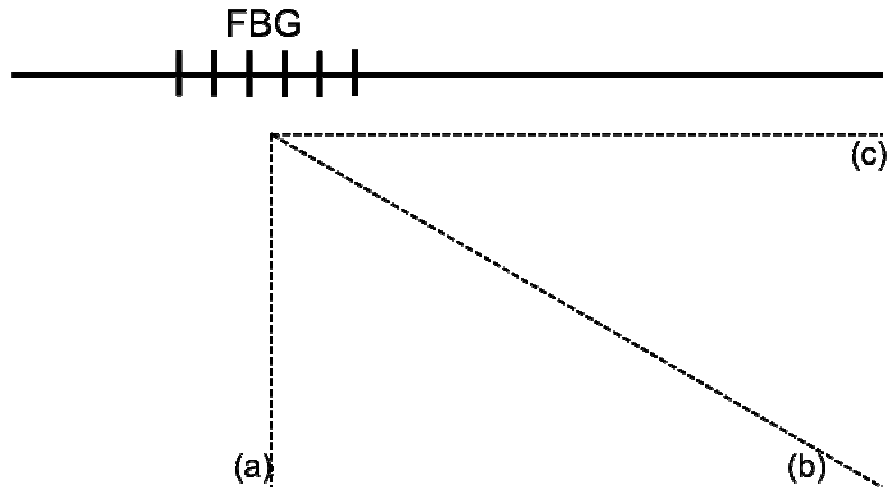


**Figure 5** A fiber grating bonded to an aluminum plate is exposed to acoustic waves generated by a transducer at three different locations

Consider a fiber grating that is bonded to an aluminum plate with a piezoelectric transducer placed in various positions along the lines a, b and c in Figure 5. The response of the fiber grating which is about 6 mm long to a 1 MHz 310 mV signal is shown in Figure 6. There are significant differences in the response depending on orientation as the acoustic wave starts to have dimensions comparable to the fiber grating.

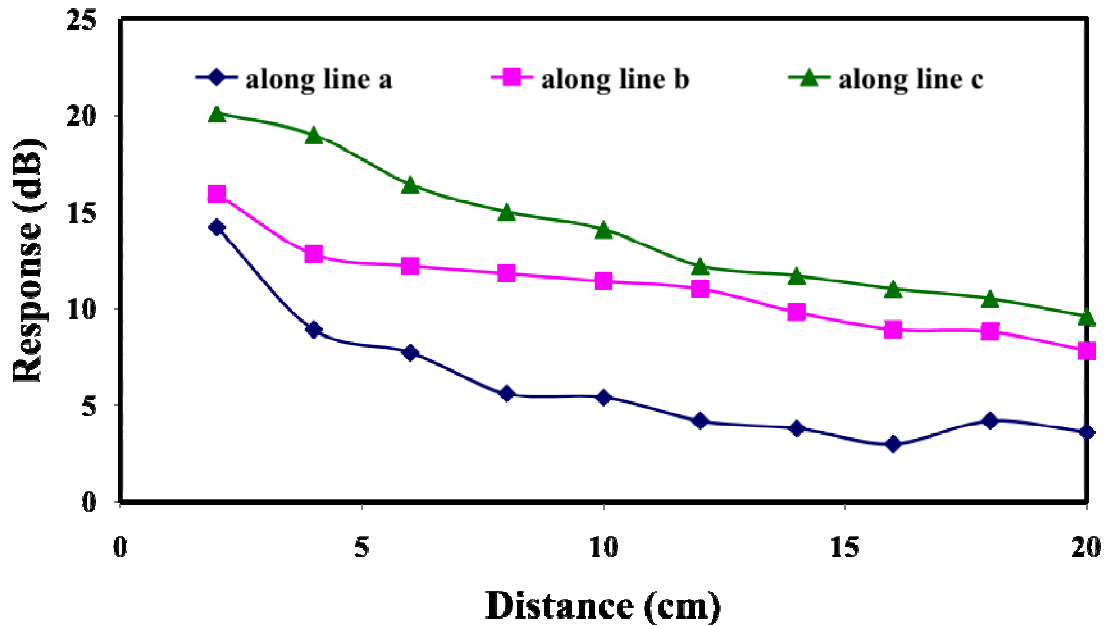


**Figure 6** Response of the FBG detector versus the distance to the ultrasonic transducer at 1 MHz. The noise floor at 310 mV is taken as the reference. Measurements were taken along three straight lines: line a – perpendicular to the grating direction; line b – 45 degrees from line a; line c – parallel to the grating direction.

At frequencies that are on the order of 30 to 40 MHz the dimensions of the acoustic wave start to have wavelengths that are on the order of the diameter of conventional optical fibers and resonances may occur when a fiber is exposed to continuous waves at a single frequency. It is possible to operate fiber grating sensors at much higher frequencies, which can be used to monitor detonations and other high-speed events.

### 3. Monitoring very high speed events - detonations

A very high-speed system involving the placement of chirped fiber gratings into energetic materials has been developed [17-21]. The detonation velocity inside or alongside the detonating high explosive can be measured with a chirped fiber-optic Bragg grating (CFBG). To show the utility of the system, a chirped fiber grating was mounted in the center of a 4-inch column of test pellets of explosive PBX-9502 shown in Figure 7. PBX-9502 was used in this experiment because its properties such density, energy and detonation velocity have been studied and are well known. The PBX-9502 test pellets and a PBX-9407 booster were placed inside an acrylic tube to maintain good alignment. A commercially made RP-1 detonator initiated the booster, which transferred the detonation into the PBX-9502 pellets. Piezoelectric pins were used to identify the position versus time of the moving detonation wave as it traveled through the pellets.

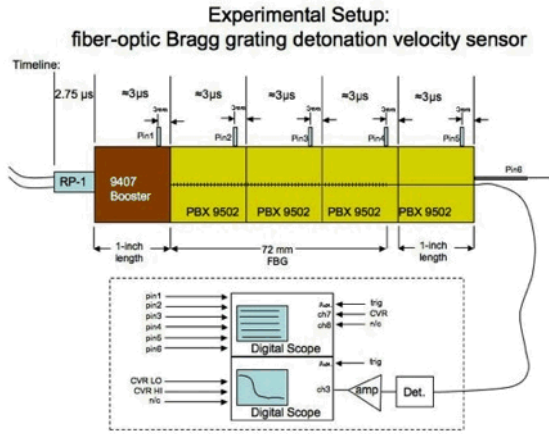


**Figure 7** Experimental setup where a CFBG is embedded in a 4-inch column of PBX-9502 (left). The detonation was initiated with a commercial RP-1 detonator followed by a 1 inch PBX-9407 booster. Five piezo timing pins were placed at 1-inch intervals along the length of the PBX-9502 column (right).

A 72-mm long CFBG was inserted into a hole down the center of the PBX-9502 pellets. The high-speed fiber grating return signal was recorded on a 500 MHz bandwidth oscilloscope. Raw results from the CFBG readout electronics are compared with simulated data, which is shown in Figure 8. The raw data was overlaid on a numerical simulation of the CFBG signal with good agreement except for the ends of the grating. The raw signal data was then analyzed to produce a plot of the position of the detonation wave versus time. The slope of the detonation position versus time gives the detonation velocity at any position along the explosive column.

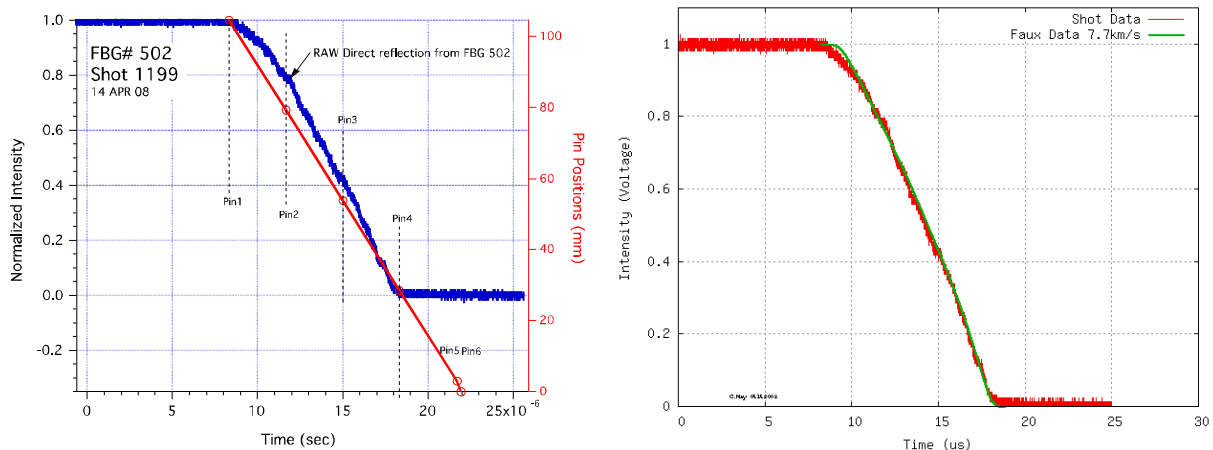


**Figure 8** Raw data from test-firing PBX-9502. Raw pin data PBX-9502 average velocity is 7.65 mm/ $\mu$ sec. Raw CFBG sensor data had good signal-to-noise ratio and agreed well when overlaid on a numerical simulation.

Indeed, after analysis, the detonation velocity was determined to be between 6.8 and 7.8 mm/ $\mu$ sec (Figure 9). This result is compared to the analysis of the simulated data, which gives 7.7 mm/ $\mu$ sec. The analyses of the real and simulated signal data agree well in the center portion of the 72 mm grating. However the agreement diverges at the ends. We think that at the ends of the grating, there is more uncertainty in the mapping of wavelength to physical position. Also, the analyzed return signal from the grating exhibits local deviations from a constant velocity, which at this point are not well explained.

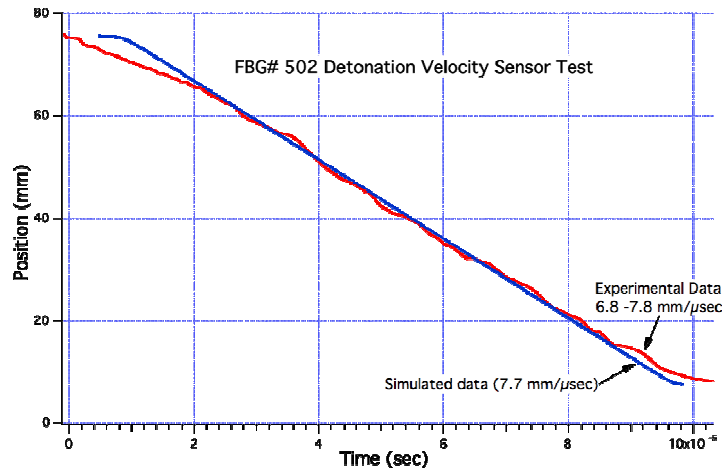


**Figure 9** The analyzed data agrees well with a simulation except at the CFBG ends.

The above experiment shows that CFBG sensor can be embedded inside a high explosive to measure the detonation velocity inside the explosive.

Three other experiments were performed to observe whether CFBG sensors could monitor detonation velocities on the exterior of a detonating explosive and also on the boundary between detonating explosives and other inert materials. In the first experiment, an 18 mm long CFBG detonation velocity sensor was placed on the surface of a 1-inch long sample of C-3 Detasheet. Detasheet is a moldable plastic explosive with applications in the mining, military and research fields.

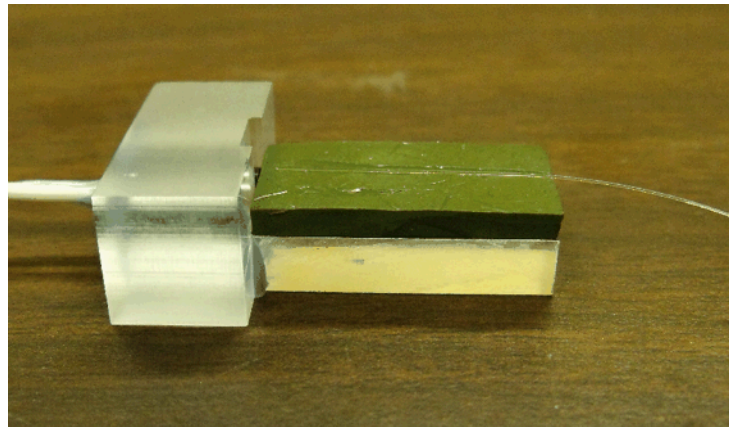


**Figure 10** An 18 mm long CFBG detonation velocity sensor was placed on the surface of a 1-inch x 0.75-inch piece of C-3 Detasheet. The Detasheet sample is affixed to a block of PMMA (acrylic plastic).

The Detasheet was initiated with a commercially available RP-2 detonator. The resulting detonation moved from the detonator into the Detasheet (from left to right in Figure 10). Using piezoelectric timing pins, the average velocity was measured to be 6.94 mm/μsec along the surface of the Detasheet sample. The CFBG-derived detonation position versus time plot is shown to the right of the raw signal plot (see Figure 11). A linear fit to the position versus time plot gives an average velocity of 6.84 mm/μsec, a 1.2% difference from the pin-derived data. Possible errors in the measurement of the length of the CFBG, and non-linearities at the grating ends could be contributing to this difference. Despite the small errors in detonation velocity, the result clearly shows that a detonation wave emerging from the side of an explosive can be continuously monitored with a CFBG attached to its



surface. We are confident that with further experimentation, the cause of the velocity differences between timing pin data and CFBG data will be explained and corrected.

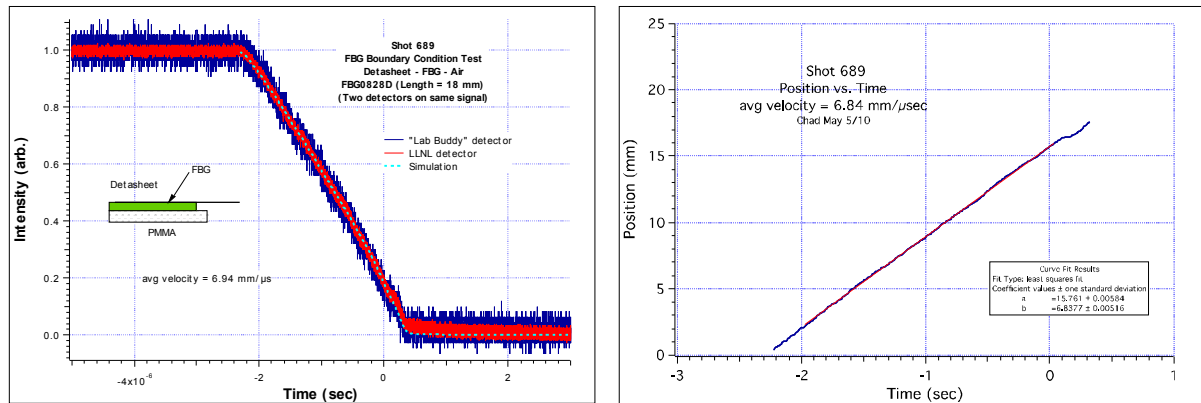


**Figure 11** The resulting raw signal data (left graph) shows the CFBG reflection intensity falling as the grating is destroyed. The analyzed data (right graph) is a position versus time plot from which the detonation velocity can be calculated.

In the second experiment, a 19 mm long CFBG was sandwiched between a C-3 Detasheet sample and a piece of 1/4 inch thick steel plate (Figure 12). The setup for this experiment is the same as for the previous experiment. The only difference is the placement of the CFBG velocity sensor; this time it was sandwiched between the Detasheet and a hardened steel base. Again, the grating sensor was able to follow the progress of the detonation wave at the explosive-steel boundary. The raw signal was analyzed and a position versus time history of the detonation wave was plotted. The slope of a linear curve fit to the position versus time plot was calculated to be 6.88 mm/μsec. Note that the piezoelectric pin average velocity measurement was slightly higher at 6.90 mm/μsec, a 0.3% difference, which is well within the uncertainty of the measurement of the length of the CFBG (see Figure 13).

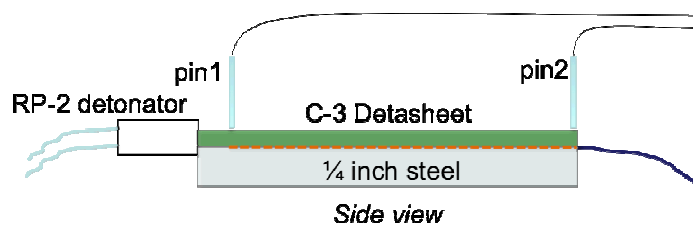
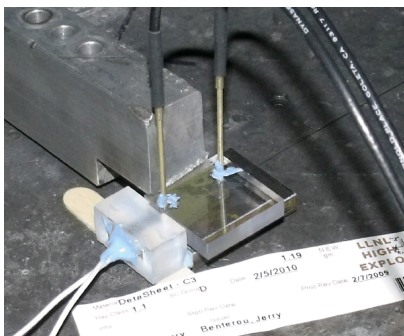


**Figure 12** The detonation velocity experiment was done inside an explosive containment vessel (left). The piezoelectric pins are used to measure the average velocity of the detonation in the Detasheet. The pin timing data agree with CFBG velocity data within 1%.

The third experiment was done to observe the detonation velocity along slots filled with a paste explosive. In the experiment, two CFBG sensors were used. One sensor (99 mm long) was placed along the length of a 100 mm long slot (0.81 mm wide and deep) filled with the paste explosive. The other sensor (134 mm long) was placed across all 4 HE-filled slots (Figure 14). The distance from slot #1 to slot #4 is 115 mm. See Figures 14 and 15 for the experimental setup.

Detonation blocks have been used to acquire a quick measurement of detonation velocity versus HE thickness and traditionally have been used with piezoelectric timing pins to simultaneously measure the average velocities of different size thicknesses of HE.

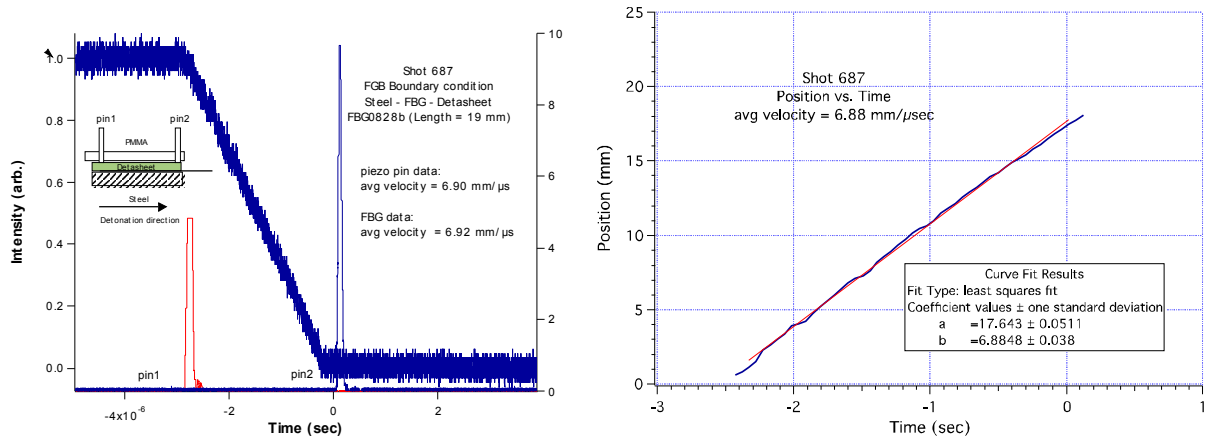


**Figure 13** Raw CFBG data (left) and position versus time plot (right) for a 19 mm long CFBG sandwiched between C3-Detasheet and hardened steel. Linear fit to the position versus time plot give a detonation velocity of 6.88 mm/μsec (6.88 km/sec).

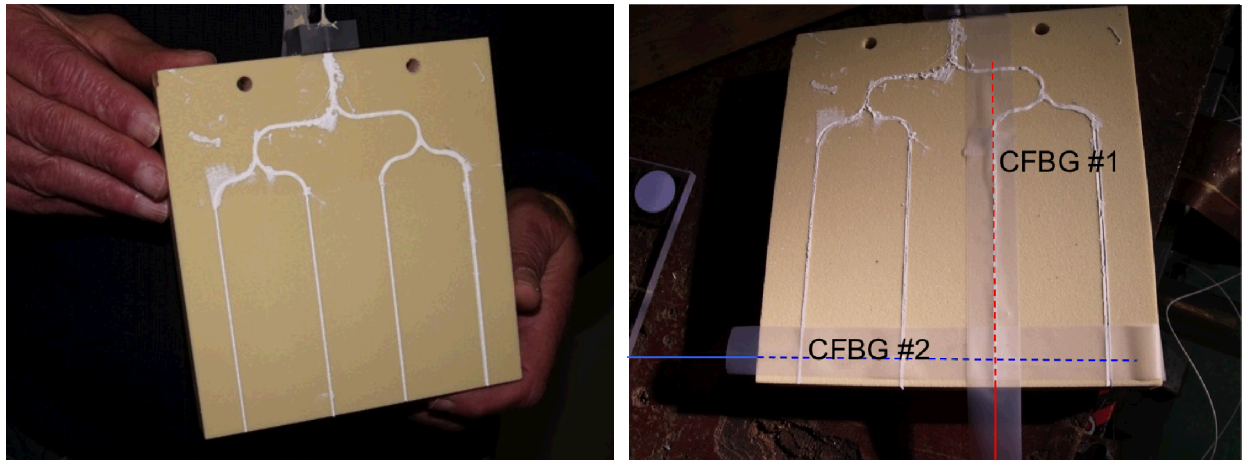


**Figure 14** A detonation block, machined from 40-lb. foam. The square slots; 0.50 mm, 0.61 mm, 0.81 mm and 1.60 mm wide and deep, respectively. The slots contain a paste explosive. The CFBG sensors were placed in the orientation shown. CFBG #1 was 98 mm long and CFBG #2 was 134 mm long.

An RP-2 detonator initiated the detonation block at a single point (Figure 15). The detonation propagated from the detonator to the first “Y” joint where it split into two, then those two detonations split into 4 parallel detonations. Pins were placed on the beginning and end of each of the four 100 mm long slots for timing marks. The two CFBG sensors were placed as described above. When the block was test-fired, the pins recorded the time difference from start to end of the straight slots, thus giving the average velocity for each slot. Subsequently, each smaller size HE slot produced a corresponding slower detonation velocity. This can be observed by analyzing the pin timing data and the return signal from CFBG #2 which was placed across the slots near the ends. Clearly the detonation in the 1.6 mm wide slot arrived first, then the detonation in 0.81 mm slot was next, and so on. Also, the energy released

was less for each subsequently smaller slot. In fact the last and smallest slot detonation was so weak, it did not appear on the CFBG sensor and it faintly appeared in the pin record. See graph in Figure 16.

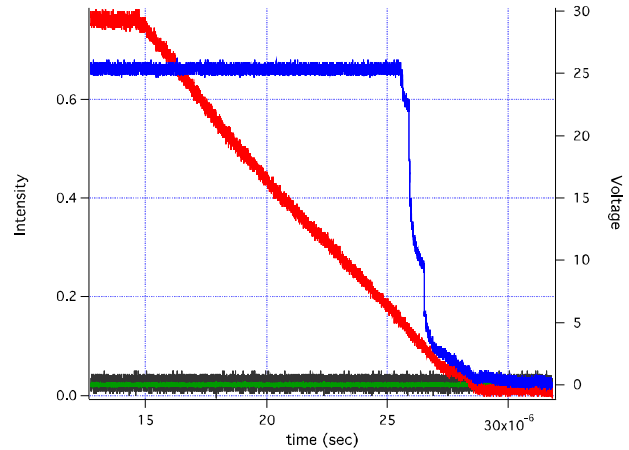
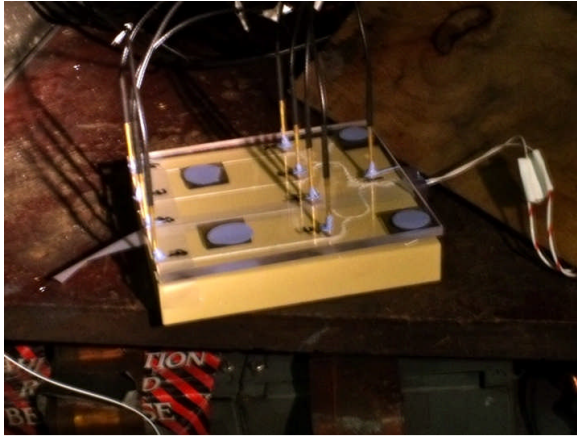


**Figure 15** Assembled explosive test-shot with pins and gratings in position before firing. Graph on right shows the resulting CFBG raw oscilloscope records. Note that the CFBG #1 (red) shows a continuous trace of the detonation wave traveling through the 0.81 mm slot. CFBG #2 (blue) was “chopped” when each of the detonations of the four slots broke the fiber at different times.

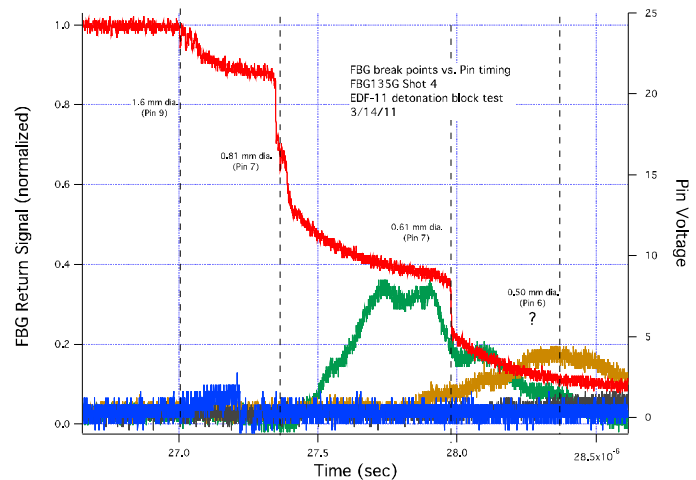
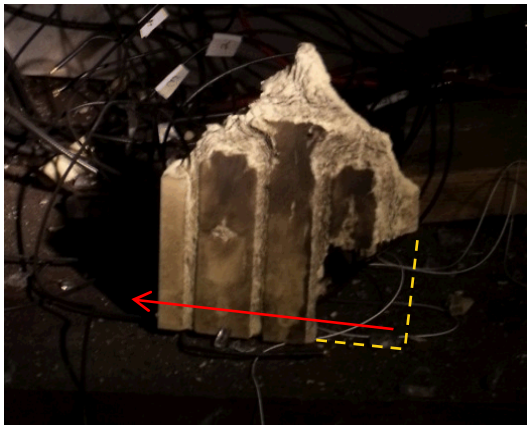


**Figure 16** A detailed look at the timing of pins and the CFBG #2 record shows good correlation. Piezo pins give better results under strong shocks and must be placed in direct contact with the explosive to produce a sharp peak.

#### 4. Analysis

We use a detector to monitor the intensity of the reflected ASE light from the CFBG. When the fiber is destroyed by the detonation wave, the reflected light extinguishes. The maximum voltage on the detector is proportional to the intensity of the returned light,

$$V_{\max} = \int ASE(\lambda)R(\lambda)D(\lambda)d\lambda \quad (1)$$

Where  $ASE(\lambda)$  is the intensity of the ASE light source,  $R(\lambda)$  is the reflectivity of the CFBG, and  $D(\lambda)$  is the response of the detector.

The maximum signal is normalized and the detector's response is flat, so this simplifies to

$$V_{\max} = 1 = \int_{\lambda_{-\infty}}^{\lambda_{+\infty}} ASE(\lambda)R(\lambda)d\lambda \quad (2)$$

As the CFBG is destroyed by the detonation wave, a fraction of the returned light is lost, so that we measure,

$$V_{meas}(t) = 1 - \int_{\lambda_{-\infty}}^{\lambda^*} ASE(\lambda)R(\lambda)d\lambda \quad (3)$$

Solving this integral for  $\lambda^*$  for each instant in time and using the linear relationship of  $x(\lambda)$  from Figure 17, we find  $x$  as a function time. Differentiation of this function gives the detonation velocity.

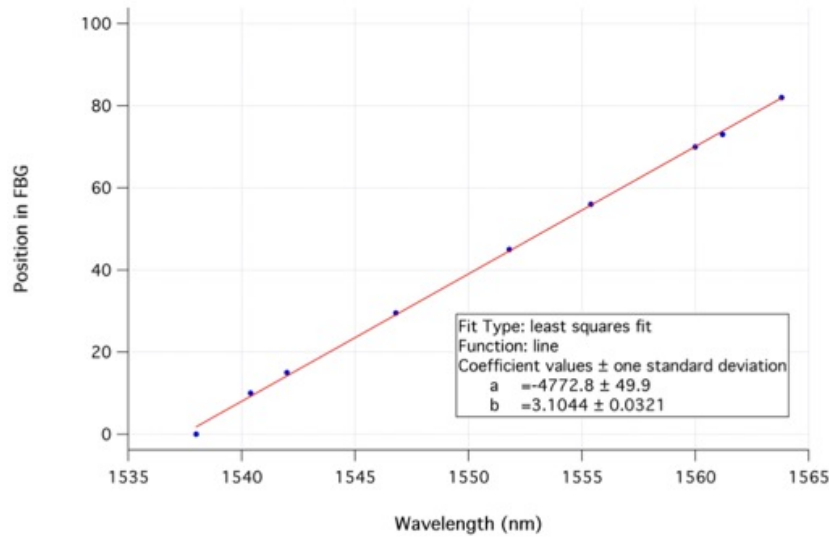


**Figure 17** This plot shows the linear relationship of position ( $x$ ) versus wavelength ( $\lambda$ ) of a typical CFBG. These data points were plotted by using a hot-tip probe to locate and map a physical location on the grating for a given wavelength value.

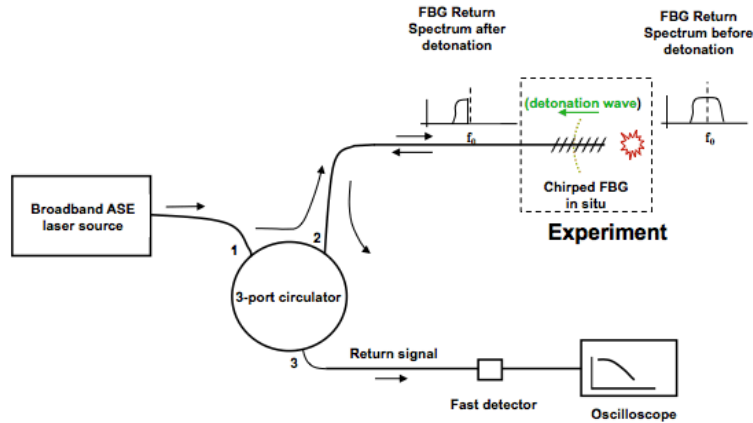


**Figure 18 Typical instrumentation for an embedded CFBG detonation velocity sensor. The detonation wave position can be monitored as it consumes the fiber grating. A position versus time history is recorded on a digitizing oscilloscope.**

## 5. Summary

Chirped fiber-optic Bragg gratings have been used as temperature and strain sensors. They can be used to support a wide variety of high-speed applications such as monitoring the structural integrity of fiberglass utility poles and roadbeds on highway bridges. Methods for monitoring ultrasound vibrations in strain fields from the 10s of kHz to 10s of MHz range were described. For most civil structure applications, systems that operate up to 5 kHz are sufficient. Ultrasonic and other nondestructive methods may require operating speeds on the order of a few MHz. It is possible to operate CFBG sensor systems at much higher speeds and applications of their usage at 100 MHz and higher were illustrated for monitoring the velocity of detonation events. Embedded CFBGs inside explosive test samples were able to track the progress of detonation waves inside the explosive. Also CFBG detonation sensors were able to track the detonation velocity of detonation waves as transit the boundaries between the explosive and air, plastic and steel. There still remains a small discrepancy between in the CFBG-derived position versus time plots on the order of 1% when compared to timing pin plots. Whether it comes from errors in CFBG length measurements or non-linearities at the CFBG ends, we are confident that with future experiments, we can resolve the cause of these errors.

## References

- [1] J.M. Seim, W.L. Schulz, E. Udd, H.M. Laylor, S.M. Soltesz, R. Edgar, "Development and Deployment of Fiber Optic Highway and Bridge Monitoring Sensor Systems", SPIE Proceedings, Vol. 3995, p. 479, 2000.
- [2] W. Schulz, J. Conte, E. Udd, J. Seim, "Static and Dynamic Testing of Bridges and Highways using Long-Gage Fiber Bragg Grating Based Strain Sensors", SPIE Proceedings, Vol. 4202, p. 79, 2000.
- [3] E. Udd, J. Seim, W. Schulz, R. McMahon, "Monitoring Trucks, Cars and Joggers on the Horsetail Falls Bridge Using Fiber Optic Grating Strain Sensors", SPIE Proceedings, Vol. 4185, p. 872, 2000.
- [4] J.M. Seim, W.L. Schulz, E. Udd, H.M. Laylor, S.M. Soltesz, R. Edgar, "Development and Deployment of Fiber Optic Highway and Bridge Monitoring Sensor Systems", SPIE Proceedings, Vol. 3995, p. 479, 2000.
- [5] W. Schulz, J. Conte, E. Udd, J. Seim, "Static and Dynamic Testing of Bridges and Highways using Long-Gage Fiber Bragg Grating Based Strain Sensors", SPIE Proceedings, Vol. 4202, p. 79, 2000.
- [6] E. Udd, J. Seim, W. Schulz, R. McMahon, "Monitoring Trucks, Cars and Joggers on the Horsetail Falls Bridge Using Fiber Optic Grating Strain Sensors", SPIE Proceedings, Vol. 4185, p. 872, 2000.

- [7] W.L. Schulz, J.P. Conte, E. Udd, J.M. Seim, "Seismic Damage Identification using Long Gage Fiber Bragg Grating Sensors", Second Workshop on Advanced Technologies in Urban Earthquake Disaster Mitigation, Kyoto Japan. July 2000.
- [8] W.L. Schulz, J.P. Conte, E. Udd, "Long Gage Fiber Optic Bragg Grating Strain Sensors to Monitor Civil Structures", Proceedings of SPIE, Vol. 4330, p. 56, 2001.
- [9] E. Udd, M. Kunzler, H.M. Laylor, W. Schulz, S. Kreger, J. Coronas, R. McMahon, S. Soltesz, R. Edgar, "Fiber Grating Systems for Traffic Monitoring", Proceedings of SPIE, Vol. 4337, p. 510, 2001.
- [10] E. Udd, S. Calvert, and M. Kunzler, "Usage of Fiber Grating Sensors to Perform Critical Measurements of Civil Infrastructure", Proceedings of OFS-16, Nara, Japan, p. 496, 2003.
- [11] S. Calvert, "High-Speed Dual-Axis Strain Using a Single Fiber Bragg Grating", Proceedings of SPIE, Vol. 5384, p. 229, 2004.
- [12] S. Calvert and J. Mooney, "Bridge Structural Health Monitoring System Using Fiber Grating Sensors: Development and Preparation for a Permanent Installation", Proceedings of SPIE, Vol. 5391, p. 61, 2004.
- [13] E. Udd, K. Corona, K. T. Slattery and D. J. Dorr, "Tension and Compression Measurements in Composite Utility Poles Using Fiber Optic Grating Sensors", Proceedings of SPIE, Vol. 2574, p. 14, 1995.
- [14] E. Udd, K. Corona, K. T. Slattery and D. J. Dorr, "Fiber Grating System Used to Measure Strain in a 22-Foot Composite Utility Pole", Proceedings of SPIE, Vol. 2721, 1996.
- [15] E. Udd, K. Corona-Bittick, J. Dorr, K.T. Slattery, "Low-cost fiber grating sensor demodulator using a temperature-compensated fiber grating spectral filter", Proc. SPIE Vol. 3180, p. 63, 1997.
- [16] I. Perez, H.L. Cui, E. Udd, "Acoustic Emission Detection using Fiber Bragg Gratings", Proceedings of SPIE, Vol. 4328, p. 209, 2001.
- [17] J. J. Benterou, E. Udd, P. Wilkins, F. Roeske, E. Roos, D. Jackson "In-situ continuous detonation velocity measurements using fiber-optic Bragg grating sensors", *Proceedings: 34th International Pyrotechnics Seminar V1*, 309-322, Beaune, France (2007).
- [18] E. Udd and J. J. Benterou, "Damage detection system with sub-microsecond resolution", Proceedings of SPIE, Vol. 6933, 2008.
- [19] J. J. Benterou, C. V. Bennett, G. Cole, D. E. Hare, C. May, E. Udd, S. J. Mihailov and P. Lu, "Embedded fiber-optic Bragg grating (FBG) detonation velocity sensor", Proceedings of SPIE, Vol. 7316, 2009.
- [20] E. Udd, J. J. Benterou, C. May, S. J. Mihailov and P. Lu, "Review of high-speed fiber optic grating sensor systems", Proc. SPIE 7677, (2010)
- [21] D. E. Hare, D. R. Goosman, K. Thomas Lorenz, and E. L. Lee, "Application of the Embedded Fiber Optic probe in high explosive detonation studies: PBX-9502 and LX-17", in *Proceedings Thirteenth Symposium (International) on Detonation*, pp. 1081-1091, Office of Naval Research (2006)

**This work performed under the auspices of the U.S. Department of Energy by Lawrence Livermore National Laboratory under Contract DE-AC52-07NA27344.**